Journal of Dental Research
1–11

DOI: 10.1177/00220345221093518
journals.sagepub.com/home/jdr

RUNX2 Regulates Osteoblast Differentiation via the BMP4 Signaling Pathway

D.D. Liu[1], C.Y. Zhang[1], Y. Liu[1], J. Li[1], Y.X. Wang[2], and S.G. Zheng[1]

Abstract

RUNX2 is a master osteogenic transcription factor, and mutations in *RUNX2* cause the inherited skeletal disorder cleidocranial dysplasia (CCD). Studies have revealed that RUNX2 is not only a downstream target of the bone morphogenetic protein (BMP) pathway but can also regulate the expression of BMPs. However, the underlying mechanism of the regulation of BMPs by RUNX2 remains unknown. In this project, we diagnosed a CCD patient with a 7.86-Mb heterozygous deletion on chromosome 6 containing all exons of *RUNX2* by multiplex ligation-dependent probe amplification (MLPA) and whole-genome sequencing (WGS). Bone marrow mesenchymal stem cells (BMSCs) were further extracted from patient alveolar bone fragments (CCD-BMSCs), an excellent natural model to explore the possible mechanism. The osteogenic differentiation ability of CCD-BMSCs was severely affected by *RUNX2* heterozygous deletion. Also, BMP4 decreased most in BMP ligands, and CHRDL1, a BMP antagonist, was abnormally elevated in CCD-BMSCs. Furthermore, BMP4 treatment essentially rescued the osteogenic capacity of CCD-BMSCs, and RUNX2 overexpression reversed the abnormal expression of BMP4 and CHRDL1. Notably, we constructed CRISPR/Cas9 *Runx2*$^{+/m}$ MC3T3-E1 cells, which simulated a variant in CCD-BMSCs, to exclude the interference of other gene deletions and the heterogeneity of the genetic background of primary cells, and verified all findings from the CCD-BMSCs. Moreover, the luciferase reporter experiment showed that RUNX2 could inhibit the transcription of *CHRDL1*. Through immunofluorescence, the inhibitory effect of CHRDL1 on BMP4/Smad signaling was confirmed in MC3T3-E1 cells. These results revealed that RUNX2 regulated the BMP4 pathway by inhibiting *CHRDL1* transcription. We collectively identified a novel RUNX2/CHRDL1/BMP4 axis to regulate osteogenic differentiation and noted that BMP4 might be a valuable therapeutic option for treating bone diseases.

Keywords: core binding factor alpha 1 subunit, bone morphogenetic proteins, CHRDL1 protein, cleidocranial dysplasia, osteogenesis, CRISPR-Cas9 systems

[1]Department of Preventive Dentistry, Peking University School and Hospital of Stomatology, National Center of Stomatology, National Clinical Research Center for Oral Diseases, National Engineering Research Center of Oral Biomaterials and Digital Medical Devices, Beijing, PR China
[2]Central Laboratory, Department of Oral and Maxillofacial Surgery, Peking University School and Hospital of Stomatology, National Center of Stomatology, National Clinical Research Center for Oral Diseases, National Engineering Research Center of Oral Biomaterials and Digital Medical Devices, Beijing, PR China

A supplemental appendix to this article is available online.

Corresponding Authors:
S.G. Zheng, Department of Preventive Dentistry, Peking University School and Hospital of Stomatology, National Center of Stomatology, National Clinical Research Center for Oral Diseases, National Engineering Research Center of Oral Biomaterials and Digital Medical Devices, No. 22, Zhongguancun South Avenue, Haidian District, Beijing, 100081, PR China.
Email: kqzsg86@bjmu.edu.cn
Y.X. Wang, Central Laboratory, Department of Oral and Maxillofacial Surgery, Peking University School and Hospital of Stomatology, National Center of Stomatology, National Clinical Research Center for Oral Diseases, National Engineering Research Center of Oral Biomaterials and Digital Medical Devices, No. 22, Zhongguancun South Avenue, Haidian District, Beijing, 100081, PR China.
Email: kqwangyx@bjmu.edu.cn

Introduction

Cleidocranial dysplasia (CCD; MIM 119600) is a rare autosomal dominant disorder that can cause developmental abnormalities of bone and teeth (Mundlos 1999). The main clinical characteristics of CCD are delayed closure of cranial sutures, hypoplastic clavicles, and multiple dental abnormalities (Mundlos 1999). *RUNX2* is the pathogenic gene of CCD, and heterozygous mutations result in the haploinsufficiency of the RUNX2 protein, affecting its normal function in skeletal development (Mundlos et al. 1997).

RUNX2, a runt domain-containing transcription factor, is essential for osteoblast differentiation and bone formation (Komori 2020). RUNX2 can upregulate the transcription of osteogenic differentiation marker genes such as osteocalcin (OCN), bone sialoprotein (BSP), alkaline phosphatase (ALP), and osterix (OSX) by binding to osteoblast-specific *cis*-acting element 2 (OSE2), which is found in the promoter regions of osteogenic genes, to promote the differentiation and maturation of osteoblasts (Ducy et al. 1997; Harada et al. 1999). In addition, RUNX2 interacts with other critical pathways, such as the TGFβ, BMP, Wnt, and FGF pathways, to regulate osteogenesis (Park et al. 2010; Chen et al. 2012; Qin et al. 2019; Chu et al. 2020). Bone morphogenetic proteins (BMPs), like RUNX2, are critical regulators of osteoblastogenesis (Salazar et al. 2016). BMP ligands initiate signaling by binding the BMP receptor complex at the cell surface. Then, 2 signaling pathways are launched by BMP receptors upon activation: the canonical Smad pathway and the Smad-independent pathway. In the canonical Smad pathway, Smad1, Smad5, and Smad9 are activated by BMP receptors, form complexes with Smad4, and translocate into the nucleus to regulate the transcription of target genes. *RUNX2* is an important BMP target gene in osteoblast differentiation and is regulated by BMPs via multiple pathways (Lee et al. 2000; Tou et al. 2003; Hassan et al. 2006; Jeon et al. 2006; Li et al. 2008; Jun et al. 2010). Some reports have also suggested that RUNX2 can influence the expression of BMPs (Choi et al. 2005; James et al. 2006; Phimphilai et al. 2006). However, the underlying mechanisms remain unknown.

Considering that CCD is a skeletal disease caused by *RUNX2* variants, it should be an excellent natural model to explore the downstream regulatory network of RUNX2 in skeletal development. This study presented a CCD patient with *RUNX2* heterozygous deletion and explored the underlying mechanism between RUNX2 and the BMP pathway in primary bone marrow mesenchymal stem cells (BMSCs) from CCD patients.

Materials and Methods

Participants

This study was approved by the Ethical Committee of Peking University Health Science Center (approval number: PKUSSIRB-2012004). An 11-y-old boy clinically diagnosed with CCD and 3 unaffected individuals participated in this study with informed consent.

Mutation Analysis, MLPA, and WGS

For mutation analysis, the exons, exon–intron boundaries, and promoter region of the *RUNX2* gene were amplified and sequenced as described previously (Quack et al. 1999; Napierala et al. 2005; Zhang et al. 2017). The multiplex ligation-dependent probe amplification (MLPA) technique was performed by the Department of Medical Genetics, Peking University Health Science Center (Beijing, China). Whole-genome sequencing (WGS) was processed using standard procedures. Details are illustrated in the Appendix.

Cell Culture and Transfection

BMSCs were isolated from the alveolar bone of the CCD patient (CCD-BMSCs) and normal donor (CON-BMSCs) during exposure of impacted maxillary central incisors for orthodontic treatment. Details about cell culture and transfection are described in the Appendix.

ALP Staining, ALP Activity Assay, Alizarin Red Staining, Western Blot Assay, and Quantitative Reverse Transcription Polymerase Chain Reaction

ALP staining, ALP activity assay, alizarin red staining (ARS), Western blot assay, and quantitative reverse transcription polymerase chain reaction (RT-qPCR) were processed according to the published work (Liu et al. 2019). Details are illustrated in the Appendix.

Generation of Runx2 Heterozygous Mutation Cell Line

CRISPR/Cas9-mediated *Runx2* heterozygous mutation in MC3T3-E1 cells was performed using the manufacturer's protocol (GeneChem). In brief, MC3T3-E1 cells were transfected with lenti-cas9 virus and selected using blasticidin (5 μg/mL; Sigma-Aldrich). Three single-guide RNA (sgRNA) oligonucleotides were constructed and seeded in MC3T3-E1/Cas9 cells, and the empty vector was used as a control. Neomycin (400 μg/mL; Sigma-Aldrich) was used to screen transfected cells. The mutation was confirmed by sequencing primarily. Then, cells were single-cell sorted using a FACS Aria II flow cytometer (BD Biosciences), seeded onto 96-well plates, and grown until each clone formed visible colonies. The obtained colonies were evaluated by sequencing for *Runx2* mutations.

Dual-Luciferase Assay

JASPAR database (http://jaspar.genereg.net/) was used to predict the binding sites of RUNX2 in the *CHRDL1* promoter region. The promoter regions of *CHRDL1* (from −2,000 to 0, from −1,750 to 0, from −1,000 to 0, from −500 to 0, and from

−110 to 0) were inserted into the pGL3-basic vector separately (named pGL3-CHL-2000, pGL3-CHL-1750, pGL3-CHL-1000, pGL3-CHL-500, and pGL3-CHL-110, respectively) by HanBio Technology Co. Ltd. The RUNX2 expression plasmid (pcDNA3.1-RUNX2) was constructed by Tsingke Biological Technology (TsingKe Biotech). pGL3-basic and pcDNA3.1-NC were the negative control plasmids. HEK293T cells were plated into 24-well plates and cotransfected with above plasmids using transfection reagent (Lipofectamine 3000 Reagent; Invitrogen). The cells were harvested 24 h after transfection, and luciferase activity was determined using a Dual-Luciferase Reporter Assay System (Promega) following the manufacturer's instructions. Luciferase activity = Firefly luciferase activity/Renilla luciferase activity (Fluc/Rluc). Relative luciferase activity = luciferase activity of the experimental group/luciferase activity of the control group.

Chromatin Immunoprecipitation Assay

Chromatin immunoprecipitation (ChIP) experiments were performed according to the manufacturer's instructions (BersinBio). Immunoprecipitation reactions were performed with antibodies against RUNX2 or IgG as a negative control. Purified DNA was then suspended for following RT-qPCR analysis. Primers are listed in Appendix Table 2. The $2^{-\Delta\Delta Ct}$ method was used to calculate the percentage of DNA target fragment relative to the input control in the ChIP reaction.

Phospho-SMAD Immunostaining of MC3T3-E1 Cells

For immunostaining experiments, MC3T3-E1 cells were plated on 8-mm diameter glass coverslips (CitoGlas) at 20,000 cells/well and incubated overnight. MC3T3-E1 cells were treated with BMP4 at 5 ng/mL alone or BMP4 plus 2.5 µg/mL CHRDL1 for 1 h. The growth medium was removed, and cells were washed with phosphate-buffered saline (PBS). Cells were fixed with 4% paraformaldehyde for 15 min. Cells were washed with PBS, then blocked and permeabilized in 50% antibody buffer/50% donkey serum and 0.3% Triton X-100 for 60 min at room temperature. Cells were washed with PBS and incubated with primary antibody phospho-Smad1/5/9 (CST) at 1:200 dilution overnight at 4°C. Cells were washed with PBS and incubated with secondary antibody, donkey anti-rabbit Alexa 647 (Jackson Immunoresearch), at 1:200 dilution in antibody buffer for 30 min at room temperature. Cells were washed with PBS and mounted with mounting medium with DAPI (Zhongshanjinqiao Biotechnology) and visualized by Leica TCS SP8 confocal microscope (Leica Microsystems).

Statistical Analysis

All experiments were repeated 3 times, and data are expressed as the mean ± SD. Student's *t* test and 1-way analysis of variance (ANOVA) were performed when appropriate. Significance is indicated as follows: $*P < 0.05$ and $***P < 0.001$.

Results

Clinical Manifestation of the CCD Patient

This study focused on a sporadic case. The patient, an 11-y-old boy, had typical CCD features, including patent fontanelles, hypoplastic clavicles, and mild scoliosis (Fig. 1A–C). Panoramic radiograph and clinical examination showed retained deciduous teeth and delayed eruption of permanent teeth and supernumerary teeth (Fig. 1D–G). Short middle phalanges of the second finger and toe, short stature, and hearing loss were also found in the patient.

Heterozygous Deletion Was Detected in RUNX2

To identify mutations in the *RUNX2* gene in the patient, sequencing analysis was first performed for the coding region, flanking intron sequences, and the promoter region (<2 kb upstream of *RUNX2*), and no mutations were found (data not shown). MLPA analysis revealed that the patient had a heterozygous deletion of all exons (exon 0 to exon 7) (Fig. 1H). WGS further clarified a 7.86-Mb deletion on chromosome 6, including the *RUNX2* gene (Fig. 1I). The deletion was confirmed by Sanger sequencing (data not shown).

Heterozygous Deletion of RUNX2 Affected the Osteogenic Ability and BMP4 Pathway in BMSCs

BMSCs were isolated from the patient and normal participant during surgical treatment of impacted teeth (named CCD-BMSCs and CON-BMSCs). Isolated cells all expressed mesenchymal stem cell (MSC) markers CD73, CD90, and CD105 and did not express leukocyte and hematopoietic markers CD45 and CD34, respectively (Fig. 2A, B). After osteogenic induction, CCD-BMSCs showed reduced ALP activity and the ability to form mineralized nodules (Fig. 2C–E). Western blot analysis revealed lower RUNX2, BSP, and OSX expression in CCD-BMSCs (Fig. 2F, G). Real-time PCR also showed that the messenger RNA (mRNA) levels of osteogenic-associated genes such as *RUNX2*, *ALP*, *BSP*, *OCN*, and *OSX* significantly declined in CCD-BMSCs ($P < 0.05$; Fig. 2H). The above results indicated that heterozygous deletion of *RUNX2* seriously interfered with the osteogenic differentiation ability of CCD-BMSCs.

The effect of *RUNX2* heterozygous deletion on BMP signaling pathways was further detected by real-time PCR. We first detected the expression of BMPs that play an essential role in osteogenesis in CCD-BMSCs and CON-BMSCs. The expression of *BMP4* was high in BMSCs, while the expression abundance of other BMPs was low (taking Ct value as reference) (Appendix Fig. 1). *BMP4* decreased significantly in CCD-BMSCs during osteogenic induction (Fig. 2I). Therefore, we speculated that the heterozygous deletion of the *RUNX2* gene seriously affected the expression of BMP4. To further explore whether RUNX2 regulates BMP4 through BMP antagonists, we detected the expression of several important BMP

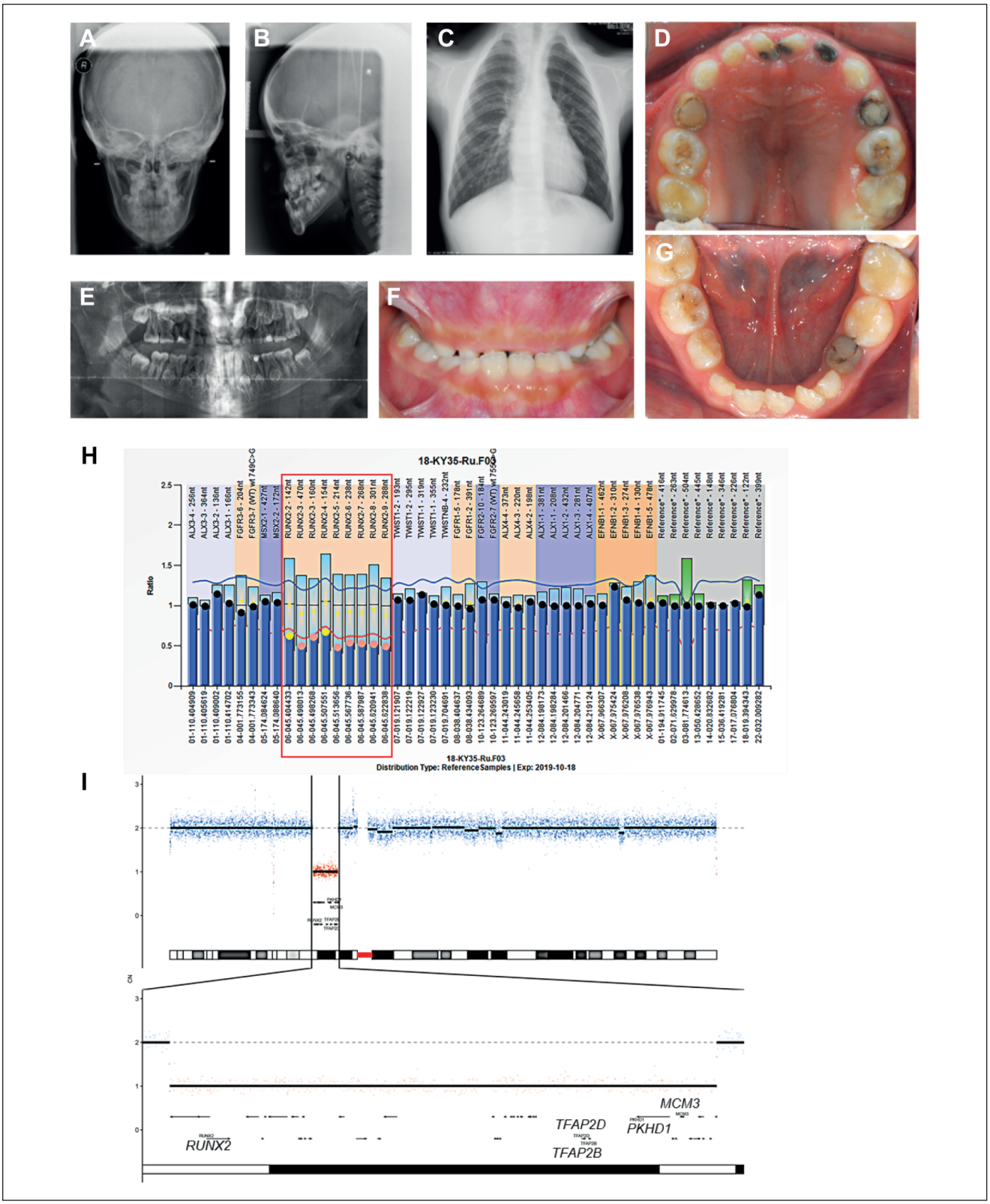

Figure 1. The diagnosis of a cleidocranial dysplasia patient with *RUNX2* heterozygous deletion. (**A**) Anteroposterior and (**B**) lateral radiographs of the skull of the proband. (**C**) Chest radiograph of the proband. (**D**) Intraoral maxillary occlusal of the proband. (**E**) Panoramic radiograph of the proband. (**F**) Intraoral center occlusal of the proband. (**G**) Intraoral mandibular occlusal of the proband. (**H**) Analysis of *RUNX2* copy number using multiplex ligation-dependent probe amplification. (**I**) Detection of the span of chromosomal deletion by whole-genome sequencing.

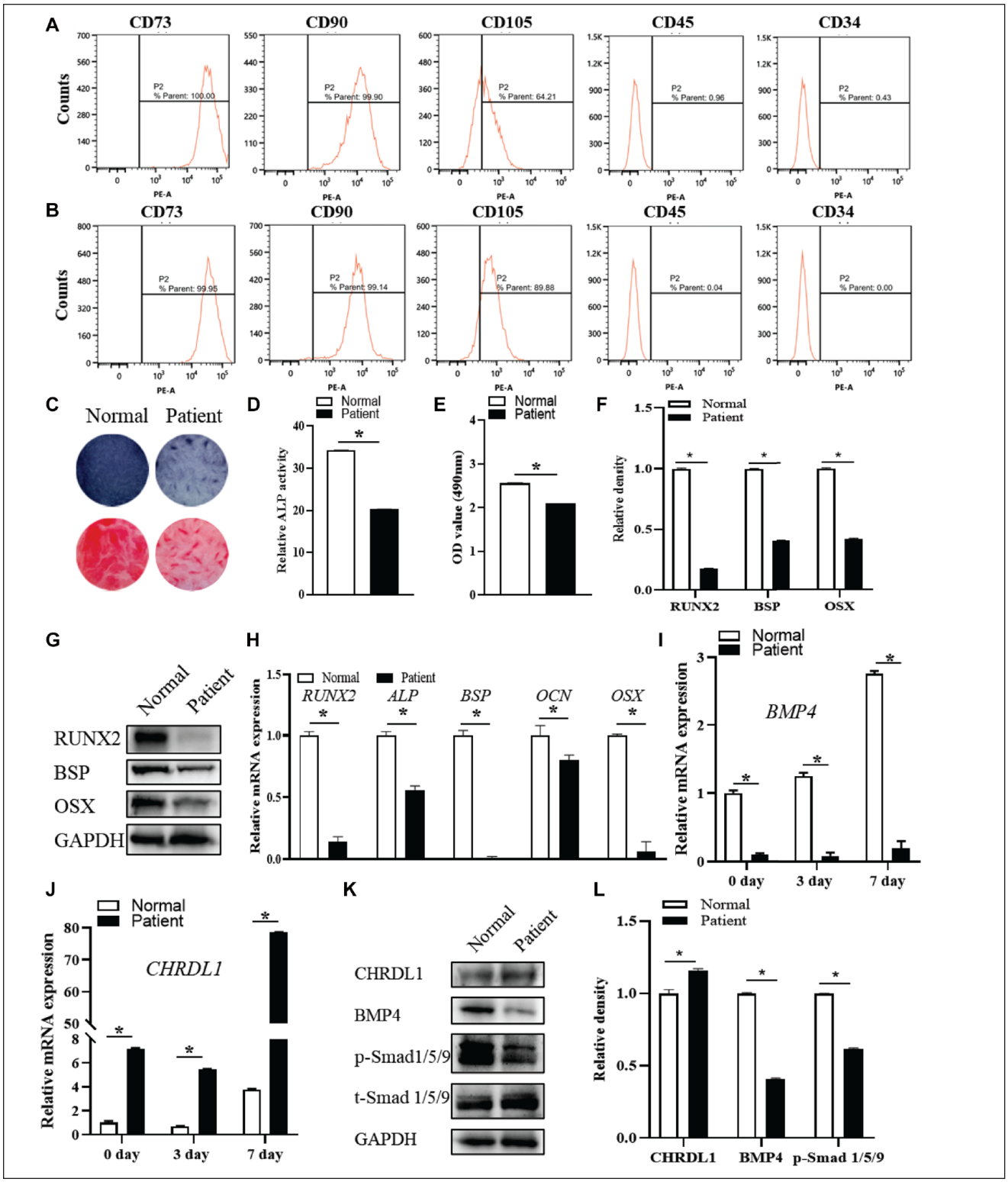

Figure 2. Heterozygous deletion of *RUNX2* interfered with the osteogenic capacity of bone marrow mesenchymal stem cells (BMSCs) and the BMP4 pathway. BMSCs from a normal control (CON-BMSCs) and a cleidocranial dysplasia patient (CCD-BMSCs) were cultured in osteogenic medium (OM). (**A**) Flow cytometric analysis showed that CON-BMSCs are positive for CD73, CD90, and CD105 but negative for CD45 and CD34. (**B**) Flow cytometric analysis showed that CCD-BMSCs are positive for CD73, CD90, and CD105 but negative for CD45 and CD34. (**C**) Alkaline phosphatase (ALP) staining and alizarin red staining (ARS) of BMSCs after induction in OM. (**D**) ALP activity was analyzed after induction in OM for 7 d. (**E**) Quantification of ARS by spectrophotometry. (**F, G**) Western blot assays analyzed the protein levels of RUNX2, BSP, and OSX in BMSCs after culture in OM for 7 d. (**H**) Quantitative analysis of the messenger RNA (mRNA) levels of *RUNX2*, *ALP*, *BSP*, *OCN*, and *OSX* in BMSCs after culture in OM for 7 d. (**I, J**) Quantitative analysis of the mRNA levels of *BMP4* (**I**) and *CHRDL1* (**J**) in BMSCs after culture in proliferation medium (PM) for 3 d or OM for 3 or 7 d. (**K, L**) Western blot assays analyzed the protein levels of CHRDL1, BMP4, and p-Smad1/5/9 in BMSCs after culture in OM for 7 d. $^*P < 0.05$.

antagonists in CCD-BMSCs and CON-BMSCs. Unexpectedly, *CHRDL1* had high expression abundance in BMSCs and significantly increased in CCD-BMSCs (Fig. 2J). The Western blot results confirmed the upregulation of CHRDL1 and downregulation of BMP4 and its downstream p-Smad1/5/9 (Fig. 2K, L). These data implied that *RUNX2* mutation prevented the BMP4 signaling pathway from exerting its effects on osteogenic differentiation.

Runx2 Mutation Caused Abnormal Osteogenesis and the BMP4 Pathway in MC3T3-E1 Cells

To exclude the effects of deletions in other genes and different cell backgrounds, we constructed a monoclonal cell line with *Runx2* heterozygous mutation in MC3T3-E1 cells by CRISPR/Cas9 technology (Fig. 3A). The mutation (c.252_310del) was validated by Sanger sequencing, which resulted in a frameshift and led to a premature protein truncated at the QA domain (Fig. 3B–D). The CRISPR/Cas9 *Runx2*$^{+/m}$ cells and CRISPR/Cas9 control cells (abbreviated as *Runx2*$^{+/m}$ cells and control cells) had normal appearance under a light microscope (Fig. 3B, C).

The ALP activity test and ARS staining revealed that, compared with control cells, the osteogenic differentiation capacity was reduced in *Runx2*$^{+/m}$ cells (Fig. 3E–G). Western blot analysis showed that the expression of RUNX2 and other osteogenic markers, including BSP and OSX, decreased in *Runx2*$^{+/m}$ cells (Fig. 3H, I). Real-time PCR revealed lower expression levels of *Alp*, *Bsp*, *Ocn*, and *Osx* ($P < 0.05$; Fig. 3J). Real-time PCR and Western blot also confirmed that the expression of CHRDL1 was elevated with reduced BMP4 and p-Smad1/5/9 expression (Fig. 3J–L). The above data illustrated that the *Runx2* mutation could impair the osteogenic differentiation capacity of MC3T3-E1 cells and damage the effect of BMP4, which was consistent with that of CCD-BMSCs.

RUNX2 Regulated Osteoblast Differentiation via the RUNX2/CHRDL1/BMP4 Axis

To further explore the mechanism of RUNX2 in the BMP4 pathway, BMP4 protein was added to CCD-BMSCs and *Runx2*$^{+/m}$ cells. As expected, BMP4 rescued the ALP activity and the capacity for mineralized nodule formation of the 2 types of cells (Fig. 4A–C). The mRNA levels of *RUNX2*, *ALP*, *BSP*, *OCN*, and *OSX* significantly increased in CCD-BMSCs, and similar results were shown in *Runx2*$^{+/m}$ cells ($P < 0.05$; Fig. 4D–H). Western blot results were consistent with those obtained by real-time PCR except BSP (Fig. 4I–L). These results confirmed that BMP4 could partly rescue the osteogenic capacity attenuated by *RUNX2* mutation and that BMP4 is a downstream target of RUNX2. We overexpressed RUNX2 in CCD-BMSCs and *Runx2*$^{+/m}$ cells and found that the elevated RUNX2 expression increased BMP4 levels and reduced CHRDL1 expression (Fig. 4M–P).

We presumed that RUNX2 had an inhibitory effect on CHRDL1 and can regulate BMP4 through CHRDL1. To verify our speculation, the effect of RUNX2 inhibition on *CHRDL1* transcriptional activity was explored. We predicted 19 RUNX2 binding sites in the promoter region (2 kb upstream of the transcription start site) of *CHRDL1* using the JASPAR database (http://jaspar.genereg.net/) (Appendix Table 3). Then, luciferase reporter experiments revealed that the range of −500 to −2,000 was responsible for transrepression of *CHRDL1* by RUNX2 ($P < 0.001$; Fig. 5A). To further determine whether RUNX2 interacted with *CHRDL1* binding sites in vivo, a ChIP assay was performed in CON-BMSCs, and the results showed that RUNX2 was most enriched on the promoter region from −500 to −1,000 (Fig. 5B). Due to the low enrichment fold, no conclusions could be drawn on the direct binding of RUNX2 to the *CHRDL1* promoter. In the immunofluorescence assay, we treated MC3T3-E1 cells with BMP4 at 5 ng/mL alone, or BMP4 plus 2.5 μg/mL CHRDL1, and found that CHRDL1 can inhibit the recruitment of p-Smad1/5/9 to the nucleus induced by BMP4 (Fig. 5C). Our findings suggest that CHRDL1 can inhibit BMP4/Smad signaling, and RUNX2 regulates the BMP4 pathway by inhibiting the transcription of *CHRDL1* in osteogenesis, while *RUNX2* mutation impairs its repressive effects on *CHRDL1* transcription (Fig. 5D).

Discussion

In this study, we uncovered a novel RUNX2/CHRDL1/BMP4 axis underlying osteogenesis. The results of osteogenic induction showed that *RUNX2* heterozygous deletion not only heavily influenced the osteogenic capability of BMSCs but also led to an abnormal BMP4 pathway. BMP4 treatment partly restored the osteogenic capacity of BMSCs, indicating that BMP4 is involved in the abnormal osteogenesis caused by the *RUNX2* mutation. Overexpression experiments, luciferase reporter experiments, and immunofluorescence revealed that RUNX2 regulates BMP4 by inhibiting *CHRDL1* transcription.

CCD is an excellent natural model for studying RUNX2 function, and CCD-BMSCs can reflect the biological effect of *RUNX2* variation more truly. Therefore, we detected the expression of BMPs and BMP antagonists in CCD-BMSCs to explore the underlying regulatory mechanism between RUNX2 and BMP signaling pathways. CRISPR/Cas9 was used to construct *Runx2* mutation monoclonal cells in MC3T3-E1 cells to eliminate the confounding effects of different cell backgrounds and other gene deletions in CCD-BMSCs. Our results showed that BMP4 is the most affected BMP ligand by *RUNX2* mutation (Appendix Figs. 1, 3). Although there are few studies on the osteogenesis of BMP4, 1 study supports our results and shows that the increase in BMP4 is greater than that of BMP2 and BMP7 after the overexpression of RUNX2 (Phimphilai et al. 2006). When we analyzed the expression of BMP pathway genes in BMSCs and CRISPR/Cas9 MC3T3-E1 cells, we found that the expression trends of some genes in the 2 cells were inconsistent (Appendix Figs. 1–4). This inconsistency may be attributable to the following reasons. First, BMSCs and MC3T3-E1 cells are 2 cells at different bone developmental

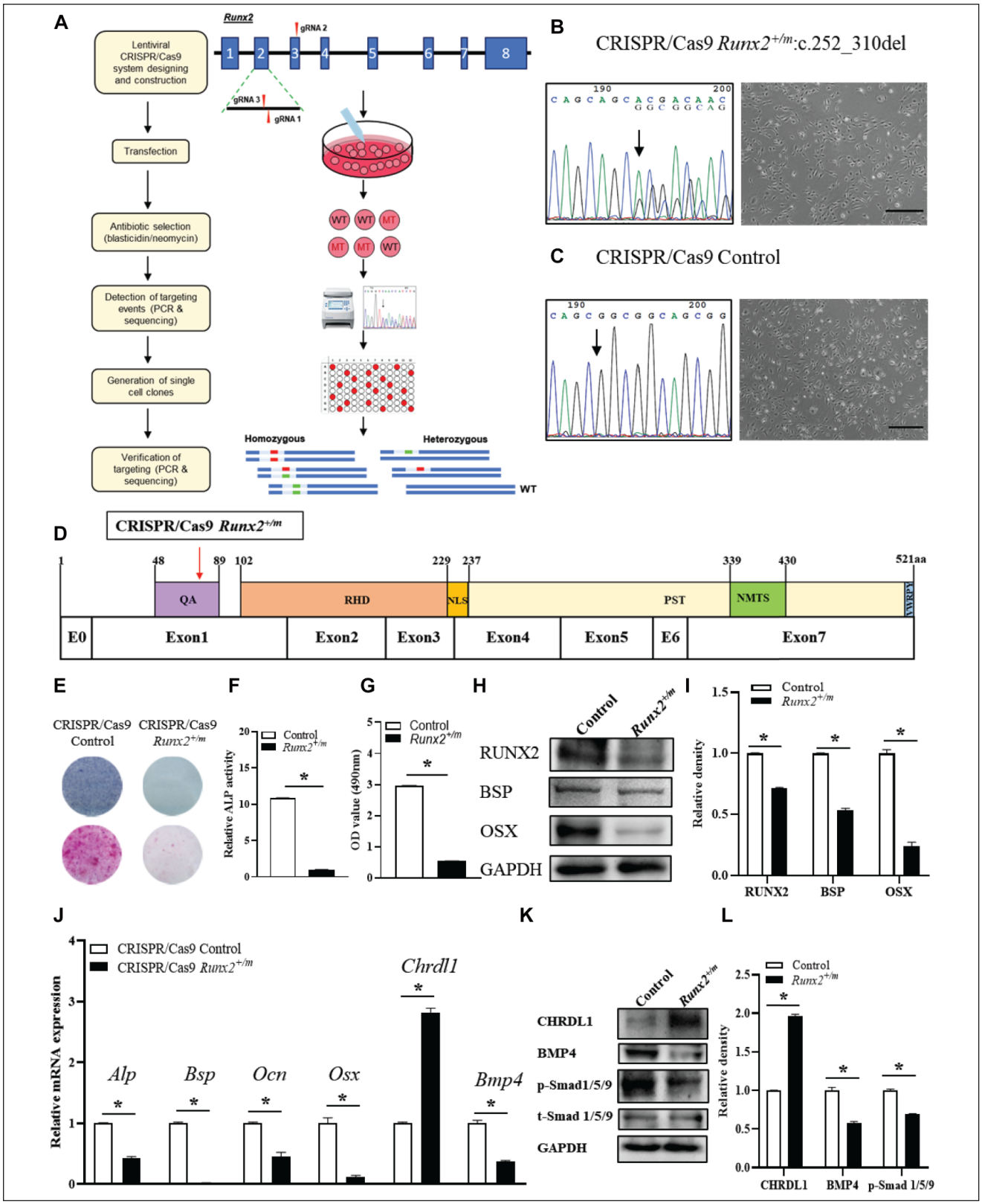

Figure 3. Heterozygous mutation of *Runx2* reduced the osteogenic ability and BMP4 pathway in CRISPR/Cas9 *Runx2*$^{+/m}$ MC3T3-E1 cells (abbreviated as *Runx2*$^{+/m}$ cells). (**A**) Flowchart of constructing a monoclonal cell line with heterozygous mutation of *Runx2* in MC3T3-E1 cells by CRISPR/Cas9 technology. (**B, C**) Sequencing analysis of *Runx2* mutation in *Runx2*$^{+/m}$ cells (B) and CRISPR/Cas9 control cells (abbreviated as control cells) (C) and detection of cell morphology under a microscope. Scale bar = 200 μm. (**D**) Schematic presentation of the location of the *Runx2* mutation. (**E**) Alkaline phosphatase (ALP) staining and alizarin red staining (ARS) of MC3T3-E1 cells after induction in osteogenic medium (OM). (**F**) ALP activity was analyzed after induction in OM for 7 d. (**G**) Quantification of ARS by spectrophotometry. (**H, I**) Western blot assays analyzed the protein levels of RUNX2, BSP, and OSX in MC3T3-E1 cells after culture in OM for 7 d. (**J**) Quantitative analysis of the messenger RNA (mRNA) levels of *Alp*, *Bsp*, *Ocn*, *Osx*, *Chrdl1*, and *Bmp4* in MC3T3-E1 cells after culture in OM for 7 d. (**K, L**) Western blot assays analyzed the protein levels of CHRDL1, BMP4, and p-Smad1/5/9 in MC3T3-E1 cells after culture in OM for 7 d. *$P < 0.05$.

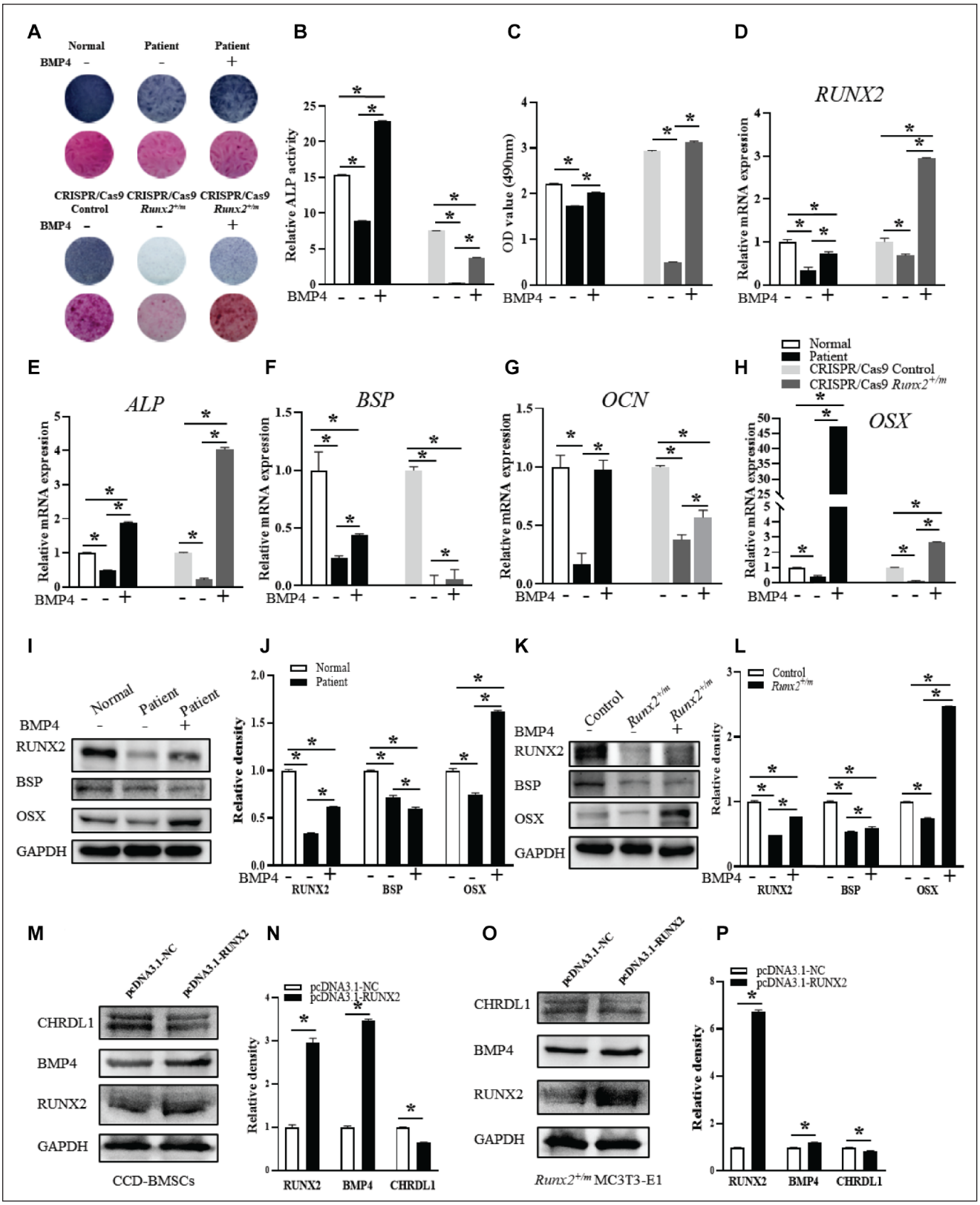

Figure 4. BMP4 treatment partially rescued the osteogenic capacity of cleidocranial dysplasia–bone marrow mesenchymal stem cells (CCD-BMSCs) and CRISPR/Cas9 *Runx2*$^{+/m}$ MC3T3-E1 cells, and RUNX2 overexpression reversed the increase of CHRDL1 expression and the decrease of BMP4 expression. BMSCs and MC3T3-E1 cells were cultured in osteogenic medium (OM) with the addition of 100 ng/mL BMP4 or an equal volume of 4 mM HCl. (**A**) Alkaline phosphatase (ALP) staining and alizarin red staining (ARS) of 2 types of cells after induction in OM. (**B**) ALP activity was analyzed after induction in OM for 7 d. (**C**) Quantification of ARS by spectrophotometry. (**D–H**) Quantitative analysis of the messenger RNA levels of *RUNX2*, *ALP*, *BSP*, *OCN*, and *OSX* in 2 types of cells after culture in OM for 7 d. (**I–L**) Western blot assays analyzed the protein levels of RUNX2, BSP, and OSX in 2 types of cells after culture in OM for 7 d. (**M–P**) Western blot assays analyzed the protein levels of RUNX2, BMP4 and CHRDL1 48 h after RUNX2 transfection in 2 types of cells. *$P < 0.05$.

stages. Also, the expression of BMP signaling components in the occurrence and development of bone and the maintenance of bone homeostasis is spatiotemporal specific (Graf et al. 2016). So, there will also be some differences in the expression of BMP signaling components in BMSCs and MC3T3-E1 cells. Second, this inconsistency may be due to differences in cell background, including species differences. Third, the expression level of some genes is low (taking Ct value as reference), which is more likely to cause fluctuations in the detection value. When analyzing the detection data of the 2 cells, we selected the genes with high expression and consistent expression trends in the 2 cells as candidate targets.

Our study further found that CHRDL1 is the mediator of RUNX2 to regulate BMP4. CHRDL1, a BMP antagonist, blocks the binding of BMPs to their receptors by competitively binding with the ligand. CHRDL1 can bind to BMP2, BMP4, BMP5, BMP6, and BMP7, of which the affinity with BMP5 and BMP6 is weak, and the affinity with BMP4 is high (Nakayama et al. 2001; Ueki et al. 2003; Chandra et al. 2006; Talavera-Adame et al. 2013; Cyr-Depauw et al. 2016). This is consistent with our findings that BMP4 had the highest differential expression among BMPs in CCD-BMSCs compared to the control. Also, our immunofluorescence experiments demonstrated that CHRDL1 could inhibit BMP4/Smad signaling in MC3T3-E1 cells.

In the luciferase assay, our results showed that when cotransfected with pCDNA3.1-NC, the luciferase activity in pGL3-CHL-1000 was lower than that in pGL3-CHL-500. This suggests that other transcription factors act on the region from −500 to −1,000 to regulate transcriptional activity. After cotransfection with pCDNA3.1-RUNX2, the luciferase activities of pGL3-CHL-110 and pGL3-CHL-500 increased, while the luciferase activities of pGL3-CHL-1000, pGL3-CHL-1750, and pGL3-CHL-2000 decreased. These results suggest that RUNX2 plays a transcriptional activation role between 0 and −500 and a transcriptional inhibition role between −500 and −2,000. This present observation may not be surprising, given that RUNX proteins are context-dependent transcription regulators (Wheeler et al. 2000). RUNX proteins act either as an activator or as a repressor by recruiting other coregulators in the promoter region of target genes. Several coregulators of RUNX2 have been identified, such as p300, SMADs as a coactivator, and histone deacetylase (HDACs), transducing-like enhancer of split (TLE) proteins, mSin3a, and yes-associated protein (YAP) as a corepressor (Zhang et al. 2000; Westendorf 2006; Krishnan et al. 2022). Whether recruitment is by a coactivator or corepressor depends on the context of transcription factor binding sites and the availability of coactivators to compete with corepressors for binding to the transcription factor (Chen and Courey 2000). So, in different regions of the *CHRDL1* promoter, RUNX2 may exert transcriptional activation or transcriptional inhibition by binding to different coregulators. It is a pity that we did not find the binding site of RUNX2 and *CHRDL1* through the

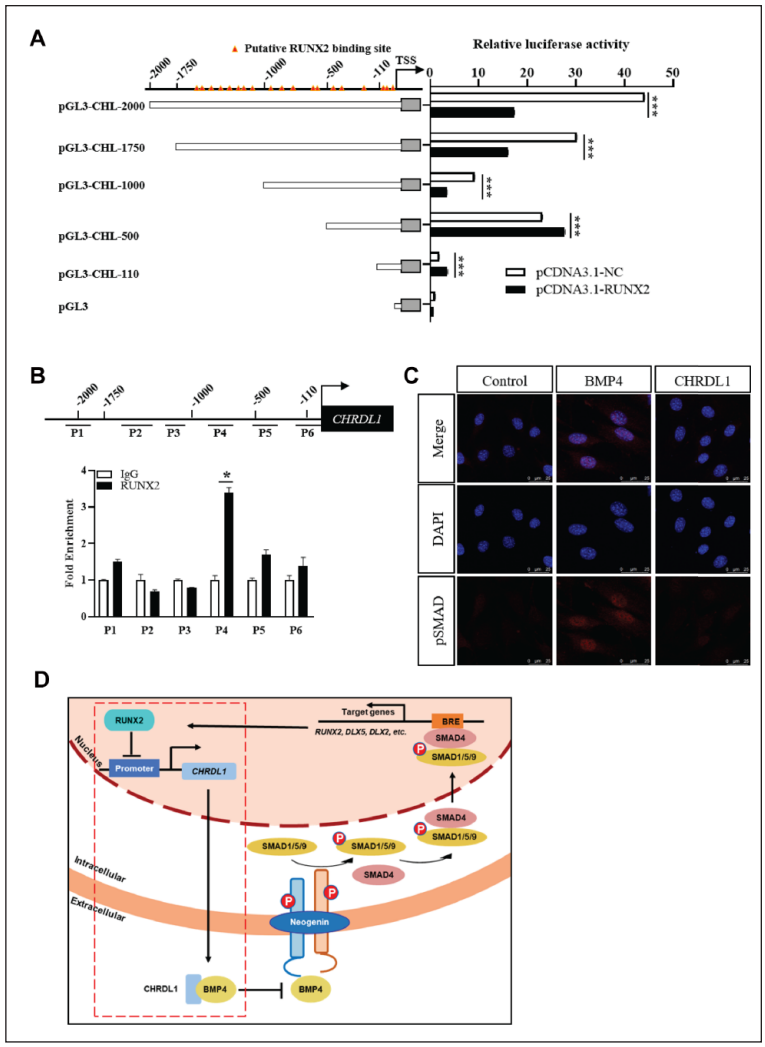

Figure 5. RUNX2 regulates osteoblast differentiation through RUNX2/CHRDL1/BMP4 axis. (**A**) Analysis of transcriptional effect of RUNX2 on the *CHRDL1*. Variable lengths of the human *CHRDL1* promoter were transfected into HEK293T cells cotransfected with Renilla luciferase and pcDNA3.1-RUNX2 (or pcDNA3.1-NC) vectors. Then, the relative luciferase activity was detected using a dual-luciferase reporter assay. (**B**) Chromatin immunoprecipitation (ChIP) assay was performed using control bone marrow mesenchymal stem cells (CON-BMSCs) with antibodies directly against RUNX2 or IgG control. Quantitative reverse transcription polymerase chain reaction was performed to analyze the immunoprecipitated DNA with primers for amplifying the sequences containing the putative RUNX2-binding sites. (**C**) CHRDL1 regulates recruitment of p-Smad1/5/9 to the nucleus in MC3T3-E1 cells. Example images of MC3T3-E1 cells treated with BMP4 at 5 ng/mL alone or BMP4 plus 2.5 μg/mL CHRDL1 for 1 h and immunostained for p-Smad1/5/9 (red) and DAPI to mark the nucleus (blue). Control means MC3T3-E1 cells without BMP4 or CHRDL1 treatment. (**D**) Schematic representation of the mechanism by which RUNX2 regulates the BMP4 pathway in osteogenesis. RUNX2 suppresses *CHRDL1* transcription and changes the antagonistic effect of CHRDL1 on BMP4. *$P<0.05$. ***$P<0.001$.

ChIP experiment. Although further studies would be required to reveal the mode of action of RUNX2 on *CHRDL1*, our current results show that RUNX2 can regulate the BMP4 pathway by inhibiting the transcription of *CHRDL1*.

In this study, BMP4 was most affected by the *RUNX2* mutation, and BMP4 treatment essentially rescued the osteogenic capacity of CCD-BMSCs. These results reveal that BMP4 may have great potential in treating bone diseases. However, only recombinant BMP2 and BMP7 have been approved by the US Food and Drug Administration (FDA) to use in several areas of orthopedics and oral and maxillofacial surgery to date (Barcak and Beebe 2017). Studies on which BMP ligand is more osteogenic are inconsistent. Some studies have shown that BMP2 is required for fracture repair and that BMP4 or BMP7 is unnecessary (Tsuji et al. 2006; Tsuji et al. 2008; Tsuji et al. 2010). Others have revealed that polymorphisms in BMP4 are associated with fracture nonunion (Guimaraes et al. 2013). In addition, a study showing that the loss of individual BMP ligands resulted in a relatively mild skeletal phenotype in mice and that the absence of multiple BMP ligands led to severe defects supports the idea that a threshold of BMP pathway activation, irrespective of specific ligands, is required to initiate ossification (Bandyopadhyay et al. 2006). Therefore, the osteogenic ability of BMPs should be explored more fully in the future, and more attention should be given to the application value of BMP4 in bone repair.

In summary, we present a CCD patient with a rare entire *RUNX2* gene heterozygous deletion. We further explored the regulatory mechanisms of RUNX2 in the BMP signaling pathway by using CCD-BMSCs and confirmed the results in CRISPR/Cas9 *Runx2*$^{+/m}$ cells. Our findings reveal a novel RUNX2/CHRDL1/BMP4 axis that regulates osteogenic differentiation in CCD syndrome. BMP4 may be a promising therapeutic target for CCD-induced bone disorder.

Author Contributions

D.D. Liu, contributed to conception, design, data acquisition, analysis, and interpretation, drafted and critically revised the manuscript; C.Y. Zhang, Y. Liu, contributed to data analysis and interpretation, critically revised the manuscript; J. Li, contributed to data acquisition and analysis, critically revised the manuscript; Y.X. Wang, contributed to conception, design, and data analysis, drafted and critically revised the manuscript; S.G. Zheng, contributed to conception, design, data analysis, drafted and critically revised the manuscript. All authors gave final approval and agree to be accountable for all aspects of the work.

Acknowledgments

We are grateful to Dr. Yu Huang (Department of Medical Genetics, Peking University Health Science Center) for *RUNX2* mutation detection strategy guidance.

Declaration of Conflicting Interests

The authors declared no potential conflicts of interest with respect to the research, authorship, and/or publication of this article.

Funding

The authors disclosed receipt of the following financial support for the research, authorship, and/or publication of this article: The study was supported by the grants from National Natural Science Foundation of China (81771053, 82001029, 81772873, 81970920).

References

Bandyopadhyay A, Tsuji K, Cox K, Harfe BD, Rosen V, Tabin CJ. 2006. Genetic analysis of the roles of BMP2, BMP4, and BMP7 in limb patterning and skeletogenesis. PLoS Genet. 2(12):e216.

Barcak EA, Beebe MJ. 2017. Bone morphogenetic protein: is there still a role in orthopedic trauma in 2017? Orthop Clin North Am. 48(3):301–309.

Chandra A, Itakura T, Yang Z, Tamakoshi T, Xue X, Wang B, Ueki T, Sato K, Uezato T, Miura N. 2006. Neurogenesin-1 differentially inhibits the osteoblastic differentiation by bone morphogenetic proteins in c2c12 cells. Biochem Biophys Res Commun. 344(3):786–791.

Chen G, Courey AJ. 2000. Groucho/TLE family proteins and transcriptional repression. Gene. 249(1–2):1–16.

Chen G, Deng C, Li YP. 2012. TGF-β and BMP signaling in osteoblast differentiation and bone formation. Int J Biol Sci. 8(2):272–288.

Choi KY, Kim HJ, Lee MH, Kwon TG, Nah HD, Furuichi T, Komori T, Nam SH, Kim YJ, Kim HJ, et al. 2005. Runx2 regulates FGF2-induced Bmp2 expression during cranial bone development. Dev Dyn. 233(1):115–121.

Chu Y, Gao Y, Yang Y, Liu Y, Guo N, Wang L, Huang W, Wu L, Sun D, Gu W. 2020. β-Catenin mediates fluoride-induced aberrant osteoblasts activity and osteogenesis. Environ Pollut. 265(Pt A):114734.

Cyr-Depauw C, Northey JJ, Tabariès S, Annis MG, Dong Z, Cory S, Hallett M, Rennhack JP, Andrechek ER, Siegel PM. 2016. Chordin-like 1 suppresses bone morphogenetic protein 4-induced breast cancer cell migration and invasion. Mol Cell Biol. 36(10):1509–1525.

Ducy P, Zhang R, Geoffroy V, Ridall AL, Karsenty G. 1997. Osf2/Cbfa1: a transcriptional activator of osteoblast differentiation. Cell. 89(5):747–754.

Graf D, Malik Z, Hayano S, Mishina Y. 2016. Common mechanisms in development and disease: BMP signaling in craniofacial development. Cytokine Growth Factor Rev. 27:129–139.

Guimarães JM, Guimarães IC, Duarte ME, Vieira T, Vianna VF, Fernandes MB, Vieira AR, Casado PL. 2013. Polymorphisms in BMP4 and FGFR1 genes are associated with fracture non-union. J Orthop Res. 31(12):1971–1979.

Harada H, Tagashira S, Fujiwara M, Ogawa S, Katsumata T, Yamaguchi A, Komori T, Nakatsuka M. 1999. Cbfa1 isoforms exert functional differences in osteoblast differentiation. J Biol Chem. 274(11):6972–6978.

Hassan MQ, Tare RS, Lee SH, Mandeville M, Morasso MI, Javed A, van Wijnen AJ, Stein JL, Stein GS, Lian JB. 2006. BMP2 commitment to the osteogenic lineage involves activation of Runx2 by DLX3 and a homeodomain transcriptional network. J Biol Chem. 281(52):40515–40526.

James MJ, Järvinen E, Wang XP, Thesleff I. 2006. Different roles of Runx2 during early neural crest-derived bone and tooth development. J Bone Miner Res. 21(7):1034–1044.

Jeon EJ, Lee KY, Choi NS, Lee MH, Kim HN, Jin YH, Ryoo HM, Choi JY, Yoshida M, Nishino N, et al. 2006. Bone morphogenetic protein-2 stimulates Runx2 acetylation. J Biol Chem. 281(24):16502–16511.

Jun JH, Yoon WJ, Seo SB, Woo KM, Kim GS, Ryoo HM, Baek JH. 2010. BMP2-activated Erk/MAP kinase stabilizes Runx2 by increasing p300 levels and histone acetyltransferase activity. J Biol Chem. 285(47):36410–36419.

Komori T. 2020. Molecular mechanism of Runx2-dependent bone development. Mol Cells. 43(2):168–175.

Krishnan RH, Sadu L, Das UR, Satishkumar S, Pranav Adithya S, Saranya I, Akshaya RL, Selvamurugan N. 2022. Role of p300, a histone acetyltransferase enzyme, in osteoblast differentiation. Differentiation. 124:43–51.

Lee KS, Kim HJ, Li QL, Chi XZ, Ueta C, Komori T, Wozney JM, Kim EG, Choi JY, Ryoo HM, et al. 2000. Runx2 is a common target of transforming growth factor beta1 and bone morphogenetic protein 2, and cooperation between Runx2 and Smad5 induces osteoblast-specific gene expression in the pluripotent mesenchymal precursor cell line C2C12. Mol Cell Biol. 20(23):8783–8792.

Li Z, Hassan MQ, Volinia S, van Wijnen AJ, Stein JL, Croce CM, Lian JB, Stein GS. 2008. A microRNA signature for a BMP2-induced osteoblast lineage commitment program. Proc Natl Acad Sci U S A. 105(37):13906–13911.

Liu Y, Sun X, Zhang X, Wang X, Zhang C, Zheng S. 2019. Runx2 mutation impairs osteogenic differentiation of dental follicle cells. Arch Oral Biol. 97:156–164.

Mundlos S. 1999. Cleidocranial dysplasia: clinical and molecular genetics. J Med Genet. 36(3):177–182.

Mundlos S, Otto F, Mundlos C, Mulliken JB, Aylsworth AS, Albright S, Lindhout D, Cole WG, Henn W, Knoll JH, et al. 1997. Mutations involving the transcription factor CBFA1 cause cleidocranial dysplasia. Cell. 89(5):773–779.

Nakayama N, Han CE, Scully S, Nishinakamura R, He C, Zeni L, Yamane H, Chang D, Yu D, Yokota T, et al. 2001. A novel chordin-like protein inhibitor for bone morphogenetic proteins expressed preferentially in mesenchymal cell lineages. Dev Biol. 232(2):372–387.

Napierala D, Garcia-Rojas X, Sam K, Wakui K, Chen C, Mendoza-Londono R, Zhou G, Zheng Q, Lee B. 2005. Mutations and promoter SNPS in RUNX2, a transcriptional regulator of bone formation. Mol Genet Metab. 86(1–2):257–268.

Park O-J, Kim H-J, Woo K-M, Baek J-H, Ryoo H-M. 2010. FGF2-activated ERK mitogen-activated protein kinase enhances Runx2 acetylation and stabilization. J Biol Chem. 285(6):3568–3574.

Phimphilai M, Zhao Z, Boules H, Roca H, Franceschi RT. 2006. BMP signaling is required for RUNX2-dependent induction of the osteoblast phenotype. J Bone Miner Res. 21(4):637–646.

Qin X, Jiang Q, Miyazaki T, Komori T. 2019. Runx2 regulates cranial suture closure by inducing hedgehog, Fgf, Wnt and Pthlh signaling pathway gene expressions in suture mesenchymal cells. Hum Mol Genet. 28(6):896–911.

Quack I, Vonderstrass B, Stock M, Aylsworth AS, Becker A, Brueton L, Lee PJ, Majewski F, Mulliken JB, Suri M, et al. 1999. Mutation analysis of core binding factor A1 in patients with cleidocranial dysplasia. Am J Hum Genet. 65(5):1268–1278.

Salazar VS, Gamer LW, Rosen V. 2016. BMP signalling in skeletal development, disease and repair. Nat Rev Endocrinol. 12(4):203–221.

Talavera-Adame D, Gupta A, Kurtovic S, Chaiboonma KL, Arumugaswami V, Dafoe DC. 2013. Bone morphogenetic protein-2/-4 upregulation promoted by endothelial cells in coculture enhances mouse embryoid body differentiation. Stem Cells Dev. 22(24):3252–3260.

Tou L, Quibria N, Alexander JM. 2003. Transcriptional regulation of the human Runx2/Cbfa1 gene promoter by bone morphogenetic protein-7. Mol Cell Endocrinol. 205(1–2):121–129.

Tsuji K, Bandyopadhyay A, Harfe BD, Cox K, Kakar S, Gerstenfeld L, Einhorn T, Tabin CJ, Rosen V. 2006. BMP2 activity, although dispensable for bone formation, is required for the initiation of fracture healing. Nat Genet. 38(12):1424–1429.

Tsuji K, Cox K, Bandyopadhyay A, Harfe BD, Tabin CJ, Rosen V. 2008. BMP4 is dispensable for skeletogenesis and fracture-healing in the limb. J Bone Joint Surg Am. 90(Suppl 1):14–18.

Tsuji K, Cox K, Gamer L, Graf D, Economides A, Rosen V. 2010. Conditional deletion of BMP7 from the limb skeleton does not affect bone formation or fracture repair. J Orthop Res. 28(3):384–389.

Ueki T, Tanaka M, Yamashita K, Mikawa S, Qiu Z, Maragakis NJ, Hevner RF, Miura N, Sugimura H, Sato K. 2003. A novel secretory factor, Neurogenesin-1, provides neurogenic environmental cues for neural stem cells in the adult hippocampus. J Neurosci. 23(37):11732–11740.

Westendorf JJ. 2006. Transcriptional co-repressors of Runx2. J Cell Biochem. 98(1):54–64.

Wheeler JC, Shigesada K, Gergen JP, Ito K. 2000. Mechanisms of transcriptional regulation by Runt domain proteins. Semin Cell Dev Biol. 11(5):369–375.

Zhang X, Liu Y, Wang X, Sun X, Zhang C, Zheng S. 2017. Analysis of novel RUNX2 mutations in Chinese patients with cleidocranial dysplasia. PLoS One. 12(7):e0181653.

Zhang YW, Yasui N, Ito K, Huang G, Fujii M, Hanai J, Nogami H, Ochi T, Miyazono K, Ito Y. 2000. A RUNX2/PEBP2alpha A/CBFA1 mutation displaying impaired transactivation and Smad interaction in cleidocranial dysplasia. Proc Natl Acad Sci U S A. 97(19):10549–10554.